Design and analysis of an integrated widely tunable laser

Andreas Hänsel, Martijn J.R. Heck

Aarhus University - Department of Engineering, Finlandsgade 22, 8200 Aarhus, Denmark

e-mail: A.Hansel@eng.au.dk

ABSTRACT

We report our work on a widely tunable laser to be used for gas sensor applications. The laser design is inspired by earlier work using an intra-cavity filter combining three asymmetric Mach-Zehnder interferometers. In our reworked design, intra-cavity losses and footprint are drastically reduced. We compare calculated outputs with data obtained from our measurements. We achieved a tuning range of more than 10 nm with output powers in the mW range.

Keywords: indium phosphide, gas spectroscopy, photonic integrated circuits, tunable laser

1 INTRODUCTION

Photonic Integrated Circuits (PICs) have the potential to replace bulk optical equipment with cheaper and smaller devices. While for some fields PICs are already the industry standard (telecom cite), only few examples for PIC-based gas sensors have been reported, despite recent publications showing their feasibility[1], [2]. We report a widely tunable laser to be used in a gas detection setup, and discuss its performance with regards to potential ammonia (NH_3) emission monitoring. The chip has been produced as part of a multi-project wafer (MPW) run to ease the technology transfer out of the lab.

2 WIDELY TUNABLE LASER

The laser design is similar to the widely tunable laser reported by Latkowski et al. in 2015[3]. It consists of three stages of asymmetric Mach-Zehnder interferometers (AMZI). This is the state of the art system for wide tuning ranges without the use of high resolution lithography needed for sampled grating distributed Bragg reflectors (SGDBRs). The original ring laser design has been replaced with a Fabry-Perot (FP) structure, where the filter elements and the semiconductor optical amplifier (SOA) are placed between two on-chip mirrors. Both designs are shown in Figure 1. In consequence, amplifier
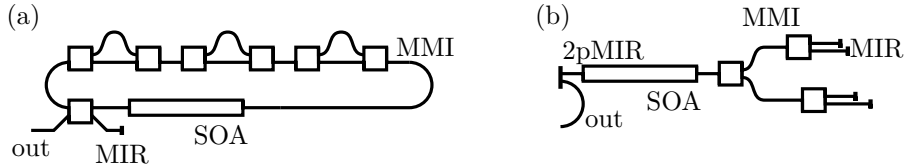

Figure 1. (a) Schematic of the ring laser in[3]. The path has been folded multiple times to make the filter section fit onto the chip. The Mach-Zehnder filter is constructed by splitting and recombining light paths with Multimode interference couplers (MMI), the gain is provided by the on-chip semiconductor optical amplifier (SOA). An MMI-reflector (MIR) is placed at the outcoupling MMI to force clockwise propagating laser light. (b) This work: Similar laser structure based on a Fabry-Perot cavity. Due to the light propagating through each active element twice per round trip, the length of the active elements can effectively be reduced by a factor two with similar performance. In addition to the elements in (a), this design uses a two-port MIR (2pMIR) to emulate a reflecting facet.

and electro-optical phase modulators (EOPMs) are passed through twice per round trip, allowing to half their footprint as compared to the ring laser design. Since SOAs and EOPMs are lossy components, this also improves the overall efficiency of the PIC. In the nested configuration, the losses due to Multimode Interference couplers (MMIs) are reduced, due to fewer light passes. This comes at the expense of a more complex tuning scheme, as the filters cannot be tuned independently and changes in one EOPM will affect multiple filters simultaneously.

2.1 Concept and tuning mechanism

In a Mach-Zehnder interferometer (MZI), light is split into two paths and subsequently recombined again, where any difference in phase leads to a difference in power transmission. In the case of AMZIs, i.e. MZIs with unequal optical path lengths in each arm, this leads to a cosine-modulated transmission

spectrum, reducing the transmission for certain wavelengths. Combining multiple AMZI, each with different arm length differences and hence free spectral ranges (FSRs), allows for tailoring the intra-cavity transmission profile of a laser cavity to select a single longitudinal mode, effectively creating a single mode laser. With proper tuning elements, this single mode laser can be tuned, potentially across the whole supported gain wavelength range. In our design, three of such filters are embedded in a FP laser cavity, with each arm containing an EOPM that allows for 2π phase tuning (double pass). A sketch of the filter design is shown in Figure 2(c), which also highlights the nomenclature for the following calculations. Photons starting from within the cavity at mirror r_1 encounter a gain section with the length L_g and MMIs, which transmit a fraction $\alpha \lesssim \sqrt{0.5}$ of the light field into each arm. Within these arms light in the top arm propagates through a waveguide of length L_t, before being split again. At the end of each arm, light is reflected with reflectivity r_2, backtracking their initial path. L_{FP} contains all the excess path length, e.g. due to waveguide bends.
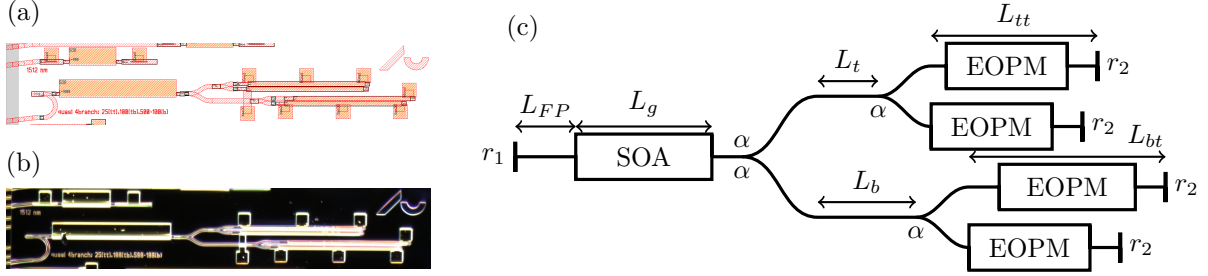

Figure 2. (a) Mask layout and (b) microscope image of the investigated circuit. (c) Sketch of the circuit along with the nomenclature of the used quantities.

During one round trip, phase and amplitude of the light with the propagation constant $\beta = n_{\text{eff}} \frac{2\pi}{\lambda_0}$ can be described by

$$q = r_1 r_2 \alpha^4 e^{2gL_g} e^{2i\beta(L_g + L_{FP})} \left[e^{2i\beta L_t} \left(e^{2i\beta L_{tt}} + e^{2i\beta L_{tb}} \right) + e^{2i\beta L_b} \left(e^{2i\beta L_{bt}} + e^{2i\beta L_{bb}} \right) \right], \qquad (1)$$

with n_{eff} as the effective index and λ_0 as the wavelength of the light. Assuming a starting field of 1, the sum of the fields from all round trips can be described by $E_{\text{total}} = \frac{1}{1-q}$ for $|q| < 1$. With E_{total} and the transmittivity t_1 through the exit mirror, the output field below the lasing threshold can be calculated. Phase shifts from the EOPMs can be implemented by adding phase terms to the corresponding elements.

2.2 Mask layout and design

The chip's layout was aligned with the design rules from SMART Photonics and made use of the standard components within this platform. Figure 2 (a) and (b) show the PIC mask design and a microscope photograph of the realized PIC. SOAs and EOPMs had a length of 1 mm, with respective arm length differences of 12.5, 75, and 400 µm. The output waveguide approached the facet under an angle and was anti-reflection coated.

3 SETUP AND MEASUREMENT METHOD

Light has been coupled from the facet of the chip to a single mode lensed fiber. Five needle probes were landed on the corresponding metal contacts on the chip; the SOA was driven with a Thorlabs ITC 8022, the EOPMs were controlled with a National Instruments NI 9264. The ground contact was on the substrate side of the chip. Light in the fiber was split with a 50/50 splitter, one output leading to an Agilent 81633A power meter, the other output leading to a Yenista OSA20.

4 RESULTS

We compared the sub-threshold output of measurement and calculation, as shown in Figure 3. The slight disagreement in both curves is due to gain curve and other device parameters not being fully implemented in the calculations yet. Those parameters will be obtained from future measurements to reach a better match of theory and measurement, and to improve on future designs. Theory and experiment showed the same free spectral range (FSR) of ~ 0.1 nm. Lasing of the laser could be shown. Lasing spectrum and current dependence are shown in Figure 4. For all the measured lines, the side mode suppression ration (SMSR) exceeded 30 dB. A treshold current of 30 mA and a tuning range of more than 10 nm could be shown. The treshold current of ring laser structure was more than twice the value reported here, despite having the same SOA geometry[3]. The narrower tuning range is a

consequence of the low current density at the lasing threshold. While this is beneficial with respect to the power efficiency of the PIC, the supported gain bandwidth is not sufficient. Increasing the current through the SOA will increase the gain bandwidth, but will lead to multi-modal behaviour. A heterodyne measurement of the laser linewidth yielded a full width at half maximum (FWHM) value of $\sim 20\,\text{MHz}$. Continuous tuning over $\sim 1\,\text{nm}$ range has been realised by changing the operating temperature of the device (15°C to 20°C). Voltage-only tuning requires additional characterisation of the device and is work in progress. For slow applications, such as environmental gas sensing, temperature tuning is feasible.
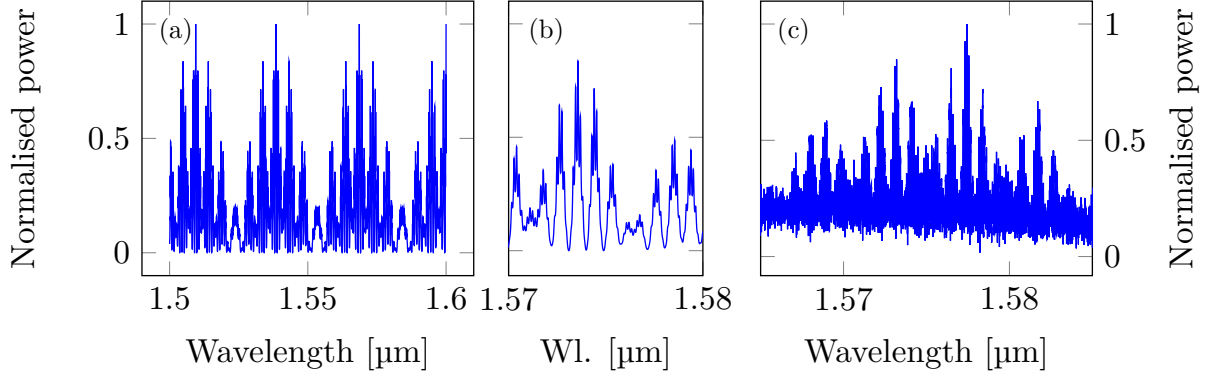

Figure 3. Normalised power spectral density. (a) Calculation, (b) zoom in on calculation, (c) measurement. In both cases, measurement and calculation, the free spectral range (FSR) was $\sim 0.1\,\text{nm}$.
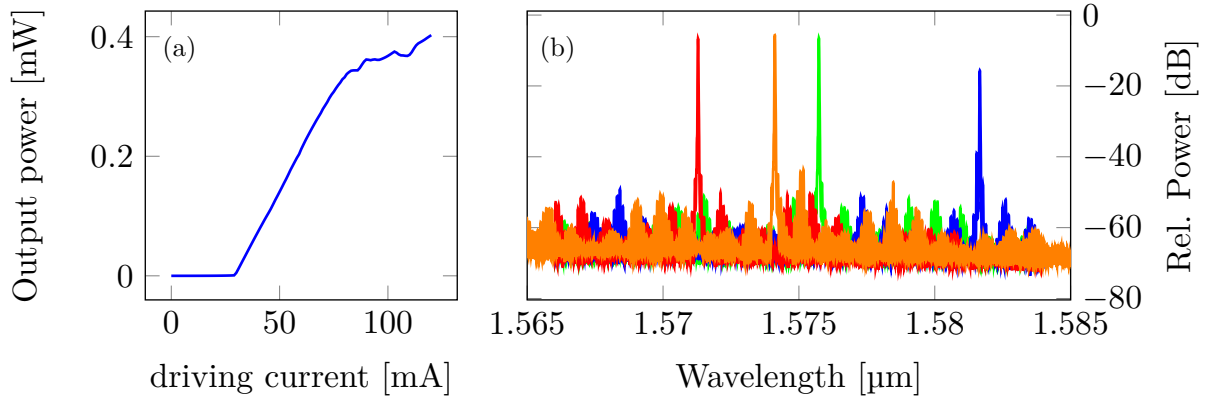

Figure 4. (a) Measured output power after fiber coupling and 50/50 splitter, (b) laser spectra for four different voltage filter settings. The side mode suppression ratio (SMSR) exceeded 30 dB.

5 CONCLUSION AND OUTLOOK

We presented our work towards a widely tunable laser to be used for gas spectroscopy. With the current configuration, more than 10 nm of tuning range could be shown, which is sufficient for multi-species gas sensing. Future work is expected to increase this tuning range and yield the device parameters required to set up continuous tuning algorithm. An increased tuning range can be achieved by increasing the threshold current density in the SOA, e.g. by reducing the SOAs length or decreasing the Q factor of the cavity. The former will further reduce the footprint, while the latter allows for additional filters in the cavity.

REFERENCES

[1] A. Hänsel and M. Heck, "Feasibility of Telecom-Wavelength Photonic Integrated Circuits for Gas Sensors," Sensors, vol. 18, 2870, 2018.

[2] L. Tombez, E. J. Zhang, J. S. Orcutt, S. Kamlapurkar, and W. M. J. Green, "Methane absorption spectroscopy on a silicon photonic chip," Optica, vol. 4, pp. 1322–1325, 2017.

[3] S. Latkowski et al., "Novel Widely Tunable Monolithically Integrated Laser Source," IEEE Photonics Journal, vol. 7, pp. 1–9, 2015.